Experiments in Fluids 12, 245–250 (1992)

Experiments in Fluids

Visualization of temperature fields and double-diffusive convection using liquid crystals in an aqueous solution crystallizing along a vertical wall

T. Nishimura

Dept. of Mechanical Engineering, Yamaguchi University, Ube 755, Japan

M. Fujiwara and **H. Miyashita**

Dept. of Materials Science and Engineering, Toyama University, Toyama 930, Japan

Abstract. This article presents a simple technique for temperature visualization using liquid crystals in an aqueous solution during the process of cooling and solidification. This method provides a clear picture of the role of double-diffusive convection in producing vertical compositional and density stratification in an initially homogeneous liquid during solidification.

1 Introduction

Natural convective flows have been known for some time to have an important influence on solidification processes involving both pure and multicomponent substances. In recent years, experimental and numerical treatments of solidification in binary systems have been stimulated by engineering applications such as crystal growth, thermal energy storage devices and the casting of metals (Beckermann and Viskanta 1988; Christenson et al. 1989, Thompson and Szekely 1989). However, numerical results have failed to achieve close quantitative agreement with experimental data for horizontal growth, unlike the solidification of a pure substance. Additional experimental and theoretical work is required for proper modelling of the transport processes of heat and species during solidification. Previous experimental studies have shown qualitative features of double-diffusive convection during solidification for various aqueous solutions (e.g., Chen and Turner 1980, Turner 1980; Turner and Gustafson 1981), but there have been few studies providing time-dependent temperature and concentration field data to test and refine mathematical modelling. This lack motivated the present investigation.

We attempt temperature visualizations of aqueous solutions during solidification along a vertical wall. The usual methods of temperature visualization, such as Mach-Zehnder and holographic interferometry, provide information about temperature variations, but they cannot be used for direct temperature measurement of aqueous solutions, because the refractive index distributions to be measured vary with both temperature and concentration.

In recent years, thermochromic liquid crystals have been adopted as a temperature-measuring probe to indicate temperature variations in several systems, particularly those involving thermal convection. Rhee et al. (1984) visualized a three-dimensional lid-driven cavity flow to study the behavior of longitudinal Taylor-Görtler-like vortices for both isothermal and naturally buoyant flows. Liquid crystal photographs gave both pathlines and temperature distribution on any lighted plane. Bergman and Ungan (1988) investigated double-diffusive convection in a two-layer, salt-stratified solution destabilized by lateral heating and cooling. Flow visualization and qualitative temperature measurements were performed with encapsulated liquid crystals. Hiller and Kowalewski (1987) and Shiina et al. (1990) also used liquid crystals to visualize flow and temperature fields of three-dimensional natural convection. A historical review of liquid crystals in heat transfer research has been presented by Moffat (1990). However, to the knowledge of the authors, no one has performed any work which uses liquid crystals to visualize flow and temperature fields during a solidification process.

Accordingly, the aim of this study is to present a simple technique of temperature visualization using encapsulated liquid crystals suspended in an aqueous solution during solidification.

2 Experimental apparatus and procedure

In the present experiment, we consider crystal growth in a super-eutectic aqueous sodium carbonate (Na_2CO_3) solution. Initially, the aqueous solution contained in a small cavity was kept at a uniform temperature ($T_i = 25\,^\circ C$) and at constant concentration ($C_i = 10$ wt%) in excess of the eutectic, and then one side wall of the cavity was cooled to the desired temperature, T_c, of $-14.6\,^\circ C$. The other walls were insulated. The height, length and width of the cavity used were $H = 50$ mm, $L = 37$ mm and $W = 30$ mm, respectively.

Liquid crystals change color according to the environmental temperature, the change being reversible and repeat-

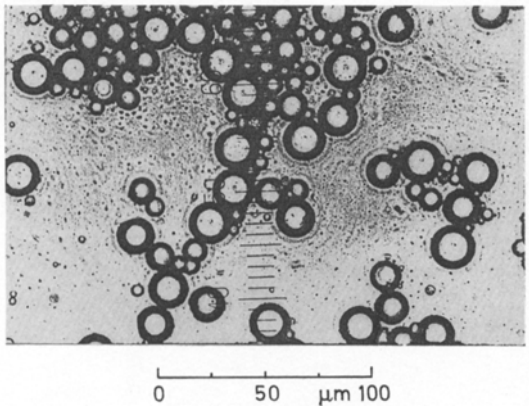

Fig. 1. Micrograph of chiral nematic liquid crystals

able as long as the crystals are not physically damaged. The liquid crystals used here were of the chiral nematics type manufactured by BDH Chemical Ltd. (Poole, England) and which were found in preliminary experiments to be stable in aqueous solutions of a number of salts. To represent two different event temperatures, we used two-event narrow-band liquid crystals, which can be made simply by physically mixing liquid crystals of the desired event temperatures. Each liquid crystal covered a temperature range of 2.5 °C, and the colors in the range from the highest to the lowest temperature included blue, green, yellow and red. The density of the encapsulated liquid crystals was about 1.02×10^3 kg/m^3, and their diameters ranged from 10 to 15 μm as shown in Fig. 1. A small amount of liquid crystals (0.004% by volume) was suspended in the aqueous solution for good visualization just before the experiment. Although the liquid crystals settled out slightly due to coagulation after being in solution, to the naked eye they appeared to be uniformly dispersed in solution 3 h after the start of the experiment. The time constant for temperature variation of the liquid crystals is about 0.2 s, and the delay in their response to temperature changes is therefore probably negligibly small for the flow fields of laminar natural convection considered here. A light beam was introduced through a slit in front of a projector lamp. Color photographs of time-dependent temperature fields were taken with an exposure time of 1 s at an angle of 90° to the plane of the incident light sheet. The temperatures were also measured with thermocouples.

3 Results and discussion

Figure 2 shows temperature variations with time at two positions, i.e., the mid-heights of the cold wall and the opposite insulated wall. The cold wall temperature falls abruptly, since the heat exchanger is suddenly exposed to the cold circulation fluid. When the temperature falls below the liquidus temperature for the initial concentration, the aqueous solution in the vicinity of the cold wall is super-

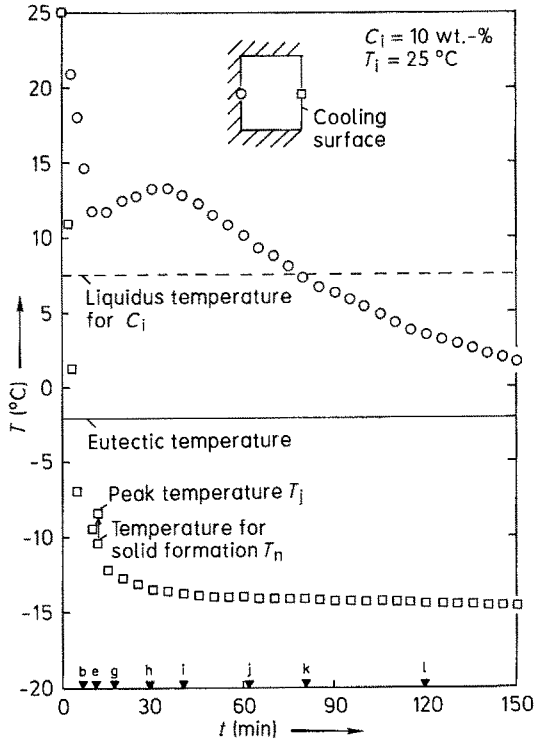

Fig. 2. Temperature histories during solidification (The points marked ▼ on the horizontal axis denote times corresponding to photographs in Fig. 3)

cooled until, at 7 min, several spike-shaped crystals of $Na_2CO_3 \cdot 10H_2O$ appear on the cold wall. At 11 min 18 s, the solid of the eutectic component is formed in the interstices among crystals near the cold wall, and the temperature jumps from $T_n = -10.4$ °C up to $T_j = -8.4$ °C due to the liberation of a large amount of latent heat. In the supercooling process, there is a marked decrease in temperature at the insulated wall. However, in the subsequent crystal growth process, the temperature increases once and decreases again. This behavior is due to double-diffusive effects as described below.

Figure 3 shows photographs of the corresponding time-dependent temperature fields revealed by two-event narrow-band liquid crystals. One liquid crystal has a working range of 2.5–5 °C, and the green color approximately indicates the 4 °C isotherm. The other has a working range of 6.5–9 °C, and the green color is approximately the 8 °C isotherm. These photographs demonstrate that the liquid crystals can be used not only to indicate temperature but also to trace fluid motion.

In the supercooling process (Fig. 3a and b), heat transfer is the only transport process. A downflow is observed in a thin cooled boundary layer and density stratification develops in the interior of the cavity. The behavior of isotherms shows that the density gradient varies smoothly, so that there is no density front between the stratified fluid and the

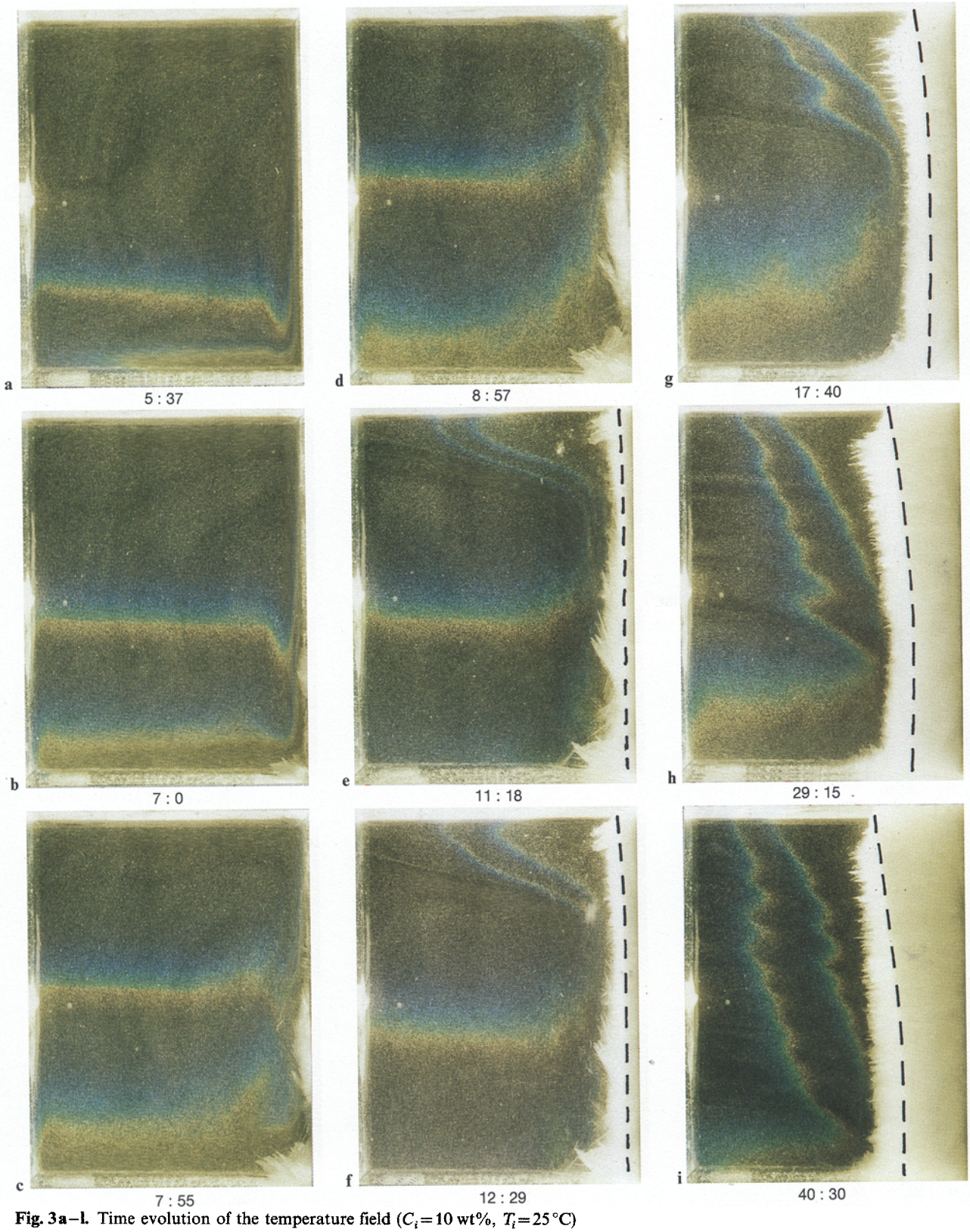

Fig. 3a–l. Time evolution of the temperature field ($C_i = 10$ wt%, $T_i = 25$ °C)

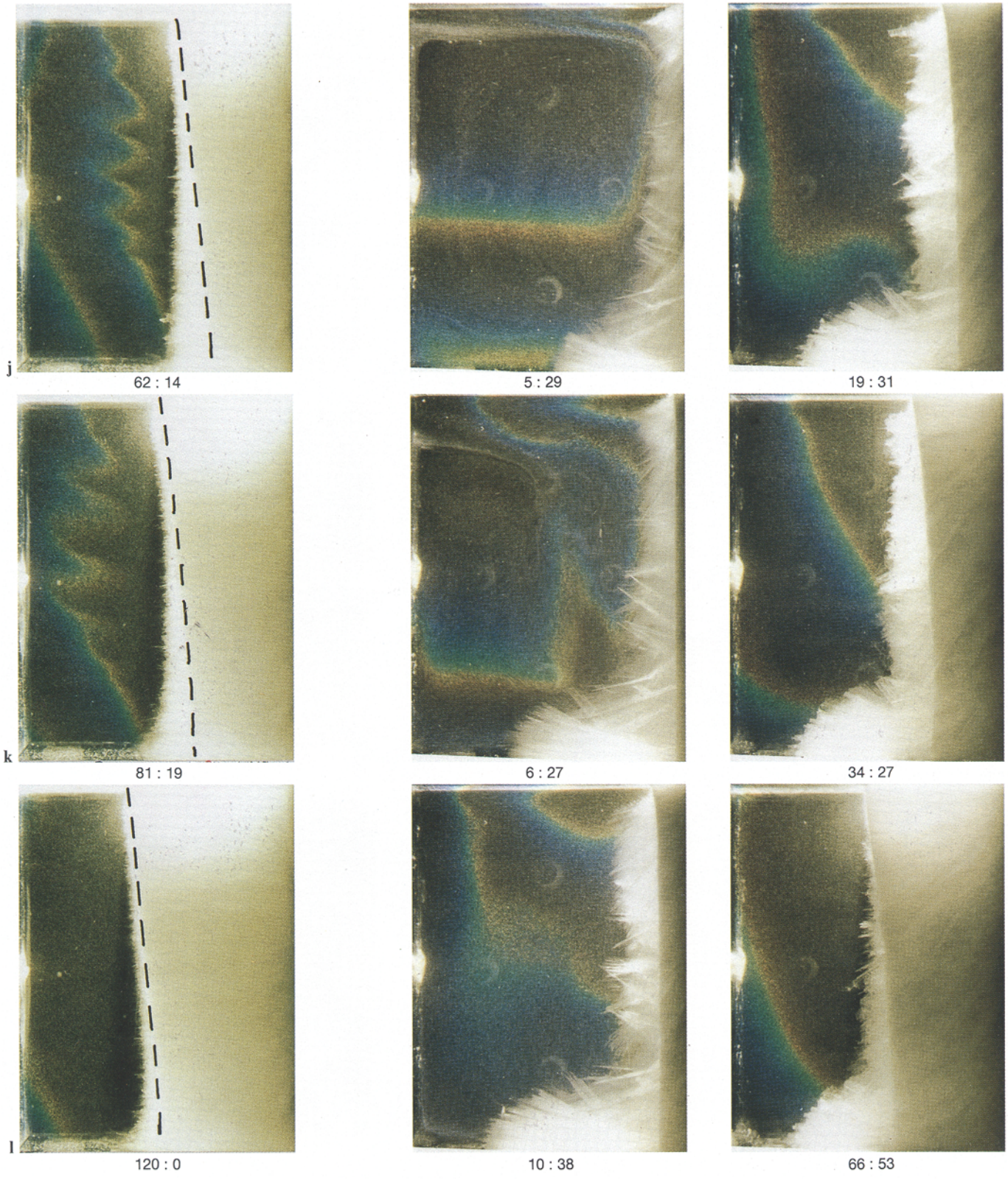

Fig. 4. Temperature field of an experiment for small initial superheating ($C_i = 12.5$ wt%, $T_i = 15\,°C$)

initially homogeneous fluid. This phenomenon has been known as the laminar filling-box process (Worster and Leitch 1985).

At the beginning of the crystal growth process (Fig. 3b–d), the crystals formed are spiky and crystallization occurs at several positions along the cold wall. Because the concentration of the initially homogeneous solution is in excess of the eutectic, the growth of crystals of $Na_2CO_3 \cdot 10H_2O$ leaves behind a more dilute fluid, less than that in the interior. The dilute fluid therefore rises along the crystal front and a vigorous upflow from each crystal is established in plumes. Note that this is solutal convection, which is upwards in spite of the fact that the fluid is cooled, thereby contrasting with the thermal convection observed in the supercooling process. Thermal convection also occurs near the crystal, and thus there is a strong interaction between the two flows, which leads to rapid variations in temperature near the crystal, as shown by the distortion of isotherms. Thus, the formation of spiky crystals leads to the initiation of the double-diffusive process.

Spiky crystals gradually cover the cold wall, and a mushy zone comprising a mixed region of liquid and crystals is formed. As the cooling progresses (Fig. 3e and f), the liquid in the interstices of the mushy zone solidifies near the cold wall, thus separating the solid zone from the mushy zone. The mush solid interface was perceptible to the eye, but poor contrast prevented its appearance on the photographs. The dotted lines were therefore inserted in the photographs to indicate its position. Now a cold dilute fluid, released by the formation of crystals, rises up through the mushy zone and accumulates at the top of the cavity, causing thermally unstable and solutally stable conditions. Therefore, there is a density front between the dilute fluid and the initially homogeneous fluid, marking the beginning of the filling-box process with double-diffusive effects (i.e., compositional stratification). It should be noted that the density front is not horizontal but tilted downwards. The behavior of the isotherms indicates that the fluid below the density front is dominated by thermal convection, but that this is damped by the compositional stratification in the fluid above the density front. Just below the density front a vigorous fluid motion is found, directed from the insulated wall towards the crystal front due to the thermal convection, which leads to a slight retardation of crystal growth in the mushy zone.

With progressing solidification, the position of the density front moves downwards and simultaneously the isotherms above the density front meander in the vertical direction, showing S-shaped temperature profiles (Fig. 3g–k). These profiles above the density front are driven by the horizontally-stacked clockwise circulations which form double-diffusive layers, and which are referred to as double-diffusive convection. The clockwise circulations are easily identified by the motion of liquid crystal particles in the magnified photographs, but are not shown here. The development of double-diffusive layers is governed by the interaction of the horizontal thermal gradient with the vertical solute stratification, although the time-dependent behavior of the system is somewhat complex. Turner (1980) was the first to visualize double-diffusive layers using a shadowgraph for a similar system, but he provided no information about temperature fields.

The photographs also reveal, firstly, that the vertical temperature gradient is reversed between the supercooling and solidifying processes, which leads to an increase of temperature as shown in Fig. 2. Secondly, the temperature at the crystal front varies with both height and time, unlike solidification of a pure substance (Fig. 3g–k). Thirdly, the fluid flow within the mushy zone is not negligible, since the shape of the mush solid interface reflects the solutal convection.

Figure 4 shows photographs of a similar experiment in which the initial superheating was small. The difference between initial and liquidus temperature is 2.6 °C in this experiment, compared with 17.4 °C in the previous one. The double-diffusive layers observed in the previous experiment are now missing. Dilute fluid continues to accumulate at the top of the cavity, creating a stable vertical solute gradient, but the horizontal thermal gradient is insufficiently conspicuous to indicate double-diffusive convection. As a result, a nearly stagnant, density-stratified region develops as solidification progresses. Thus, the development of the vertical density stratification in the interior of the cavity leads to the establishment of either a stagnant region in the liquid or double-diffusive layers. The condition under which double-diffusive convection is important is probably controlled by both the initial superheating and the initial concentration which represent the strength of the thermal effect and of the solutal effect, respectively. This will be investigated in the future.

4 Summary

A simple technique for temperature measurement by use of liquid crystals is much more helpful in interpreting the double-diffusive process during solidification of a binary system than such conventional techniques as thermocouples, although the temperature range for measurements is limited. Moreover, it seems worth comparing the experimental results obtained here with the isotherms obtained by numerical calculation, to evaluate the mathematical modelling of the solidification of binary systems.

Acknowledgements

The authors would like to thank the referees of this journal for useful suggestions in improving the original version of this paper.

References

Beckermann, C.; Viskanta, R. 1988: Double-diffusive convection during dendritic solidification of a binary mixture. Physicochem. Hydrodynam. 10, 195–213

Bergman, T. L.; Ungan, A. 1988: A note on lateral heating in a double-diffusive system. J. Fluid Mech. 194, 175–186

Chen, C. F.; Turner, J. S. 1980: Crystallization in a double-diffusive system. J. Geophys. Res. 85, 2573–2593

Christenson, M. S.; Bennon, W. D.; Incropera, F. P. 1989: Solidification of an aqueous ammonium chloride solution in a rectangular cavity. II. Comparison of predicted and measured results. Int. J. Heat Mass. Transfer 32, 69–79

Hiller, W. J.; Kowalewski, T. A. 1987: Simultaneous measurement of temperature and velocity fields in thermal convective flows. In: Flow Visualization IV (ed. Veret, C.), 617–622. Washington: Hemisphere

Moffat, R. J. 1990: Some experimental methods for heat transfer studies. Exp. Therm. Fluid Sci. 3, 14–32

Rhee, H. S.; Koseff, J. R.; Street, R. L. 1984: Flow visualization of a recirculating flow by rheoscopic liquid and liquid crystal techniques. Exp. Fluids 2, 57–64

Shiina, Y.; Akino, N.; Kunugi, T.; Fujimura, K. 1990: Visualization of flow and temperature fields of natural convection in a hemisphere heated from below. J. Flow Visualization Soc. Jpn. 10, 41–46

Thompson, M. E.; Szekely, J. 1989: Density stratification due to counterbuoyant flow along a vertical crystallization front. Int. J. Heat Mass Transfer 32, 1021–1036

Turner, J. S. 1980: A fluid-dynamical model of differentiation and layering in magma chambers. Nature 285, 213–215

Turner, J. S.; Gustafson, L. G. 1981: Fluid motions and compositional gradients produced by crystallization or melting at vertical boundaries. J. Volcanol. Geothermal, Res. 11, 93–125

Worster, G.; Leitch, A. M. 1985: Laminar-free convection in confined regions. J. Fluid Mech. 156, 301–319

Received July 22, 1991